High Accurate Positioning Technique for AUV

TAIN-SOU TSAY
Department of Aeronautical Engineering
National Formosa University
64, Wen-Hua Road, Huwei, Yunlin, 63208
TAIWAN
tstsay@nfu.edu.tw

Abstract: -In this paper, a high accurate positioning technique is proposed for autonomous underwater vehicle(AUV). It needs not position correction from Global Position System (GPS) above the sea surface and short- or long-baseline acoustic positioning system(SBL or LBL) under the sea. Two long time experiments gave maximal and average deviations are less than 33.6m and 15.1m; respectively. Position deviations are verified by tracking datum of a long-baseline acoustic position system with post navigation processing datum. These deviations are much less than the tracking range of sonar. High accurate positioning results let vehicles have less supporting from launching vessel and give flexible and mobile operations.

Key-Words: -Position estimation, Navigation and guidance, Autonomous underwater vehicle.

1 Introduction

Two types of unmanned underwater vehicles are in use: Remotely Operated Vehicle (ROV) and Autonomous Underwater Vehicle (AUV). ROVs are teleoperated through a cable, which supplies power to the vehicle. The drag on the cable and power transmission losses through the cable increase with increase in the operating range of the vehicle. AUVs do not have such limits, and have a wide scope of operation as they carry their power supply onboard. As there is no external communication for guidance, and power available is limited, mission planning and navigation are extremely critical for successful operation of AUVs. Unmanned underwater vehicles are used to perform exploration, survey, monitoring and data collection task that reduce ship cost and human risks [1].

Generally navigation requirements for survey AUV [2] are (1) mission programming to follow a predetermined survey area (or survey grid) load to the AUV; (2) mission positioning accuracy of 10 to 40 meters; (3) data positioning accuracy of 5 to 20 meters; (4) capable of using position updated from acoustic positioning, e.g. short-baseline (SBL) or long-baseline (LBL) positioning systems [3, 4] transmitted from the support vessel, seabed beacons; (5) preferably capable of using position updates form global position system (GPS) when on the sea surface [5, 6].

The position of the AUV stated above plays a central role in guidance and control for engaging or searching underwater targets. This is due to the short-range detection of sonar in noisy environment or water clarity for imaging sensors(camera) and there is no position correction technique can be applied from surface (e.g., GPS) for inertial navigation system (INS). The GPS is widely used for positioning above the sea surface. However, the strength of the electromagnetic wave from GPS satellite is decayed rapidly in the water. Therefore, GPS is not applicable in the deep water. However, the initial position of the AUV can be corrected by GPS before launch and give good mission plan positioning accuracy.

Similar to the positioning techniques of the GPS, the LBL (or SBL) is normally used for submersed vehicles [3, 6]. The sound wave replaces the electromagnetic wave for distance measurements. It needs one transponder in submersed vehicle and at least other three transponders mounted on the seabed. The distances between transponders are dependent on the power of the acoustic signal and may be up to 14000m [4]. The accuracy of the LBL may up to 5m with positions of transponders are corrected by GPS. However, the LBL system is hard to install and maintain. It needs long time to install and recovery transponders on the new operating area. The operating time and range of transponders are limited from the capacity of battery. Therefore, good position accuracy of the

underwater vehicle without LBL is generally expected for flexible and mobile applications. Note that it is impossible to install the LBL system on the battlefield for military applications.

Position datum of the on-board INS is generally not applicable after long-time operation (e.g., >1hour). This is due to senor device alignment accuracy, gyro drift, and accelerometer accuracy. Maximal detection range of the on board active sonar for compact vehicle in deep water is about 2000m. The detection range may be reduced to be about or less than 200m in the shallow water [7, 8]. Corresponding to 2000m deviation in one hour, typical specifications of the INS[5] are: (a) Installation accuracy (3σ): rolling, pitching and yawing axes in 0.005deg; (b) Gyro accuracy (3σ): bias drift in 0.005deg/hr; (c) accelero-meter accuracy (3σ): 0.03mg. They are expensive. In this work, chipper components with accuracies reduced order one will be used. Since the vehicle depth can be measured by the depth meter, therefore much attention is paid for lateral deviations. Lateral deviations due to rolling gyro drift, rolling installing error, and accelerometer accuracy versus time t are function of t^3, t^2, t^2; respectively. Therefore, pure INS without correction becomes not applicable after long-time operation. Another unpredictable parameter for positioning is the sea current. It is dependent on the moon and wind. For example, constant 0.5m/s (~1knot) current gives ~1800m position deviation after one hour. It is usually greater than the detection range of the active sonar [8]. Therefore, other stable positioning techniques must be applied to get a non-diverging position datum for AUV operations.

Rolling speed of the propelling motor, depth measurement of depth meter, estimated current information and low-cost rate gyros and accelerometers with state observers will be used to estimate the vehicle position. The attitude angles are low drift datum (e.g., 0.05deg/hr). The accuracy of depth meter is between 5cm and 50cm. The vehicle steady-state speed is proportional to the rolling speed of the propelling motor. Depth measurement and motor rolling speed are two bounded data. Experiments for verifying the proposed positioning method are performed. The operation time is 783sec. The vehicle was tracked by LBL. The proposed method gave maximal deviation is equal to 33.6m and average deviation is equal to 15.1m with respect to LBL tracking datum. However, the INS gives 524m deviation. Another 1176sec experiment gave maximal deviation is equal to 25.6m and average deviation is equal to 11.8m. These deviations are much less than the tracking range of the sonar. Therefore, the proposed method lets the AUV become a real autonomous vehicle system with less supporting from launching vehicle.

This paper is organized as follows: Section 2 describes the considered AUV, equations of motion, evaluates the small signal dynamic models and propelling model for 6-DOF simulations and autopilot designs; Section 3 performs the adaptive autopilot designs; Section 4 proposes the positioning techniques; Section 5 gives the experimental and comparison results.

2 System description and small signal dynamic modeling

Fig.1 shows the configuration and coordinate definitions of the considered underwater vehicle. The physical dimension is compatible to that of the MK-48 torpedo (579cm long; 53.3cm diameter; 1545kg weight). The central of gravity (CG) is 5.4cm below the central of buoyancy (OB). Therefore, the rolling axis is inherent stable and major control efforts are paid for pitching/yawing controls. The front propeller has seven leaves and rear propeller has five leaves. They are actuated by two counter direction electric motors for rolling torque balance.

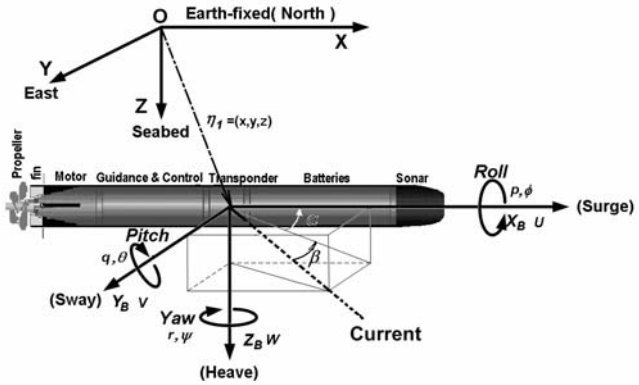

Figure 1. Coordinate system of the underwater vehicle.

Equations of motion are generally derived in the body coordinate frame. In this work, the mass, added mass and damping matrices are assumed be diagonal. Equations of motion of an underwater vehicle in six degree of freedom (6DOF) can be

written as in the form of [9]

$$\begin{aligned}
&\dot{\eta}_1 = J_1(\eta_2)v_1 \\
&\dot{\eta}_2 = J_2(\eta_2)v_2 \\
&M_1\dot{v}_1 = -C_1(v_1)v_2 - D_1(v_1)v_1 + \tau_1 \\
&M_2\dot{v}_2 = -C_1(v_1)v_1 - C_2(v_2)v_2 - D_2(v_2)v_2 - g_2(\eta_2) + \tau_2
\end{aligned} \tag{1}$$

where $\eta_1 = [x \quad y \quad z]^T$, $\eta_2 = [\phi \quad \theta \quad \psi]^T$, $v_1 = [u \quad v \quad w]^T$, $v_2 = [p \quad q \quad r]^T$. The symbols ϕ, θ, ψ p, q and r denote the roll, pitch and yaw angles and angular rates while *x, y, z, u,* v and *w* are the surge, sway and heave displacements and velocities; respectively. The terms $J_1(\eta_2)$, $J_2(\eta_2)$, M_1, $C_1(v_1)$, $D_1(v_1)$, M_2, $C_2(v_2)$, $D_2(v_2)$ and $g_2(\eta_2)$ denote the kinematical transformation, mass, Coriolis, damping matrices including the added mass effect, and the restoring vector, respectively. The kinematical transformation matrices in roll, pitch, and yaw are defined as

$$J_1(\eta_2) \equiv \begin{bmatrix} c\theta c\psi & s\phi s\theta c\psi - c\phi s\psi & c\phi s\theta c\psi + s\phi s\psi \\ c\theta s\psi & c\phi c\psi + s\phi s\theta s\psi & c\phi s\theta s\psi - s\phi c\psi \\ -s\theta & s\phi c\theta & c\phi c\theta \end{bmatrix} \tag{2}$$

$$J_2(\eta_2) \equiv \begin{bmatrix} 1 & s\phi t\theta & c\phi t\theta \\ 0 & c\phi & -s\phi \\ 0 & s\phi / c\theta & c\phi / c\theta \end{bmatrix} \tag{3}$$

where $c\bullet = cos(\bullet)$, $s\bullet = sin(\bullet)$ and $t\bullet = tan(\bullet)$. The mass matrices are

$$\begin{aligned}
&M_1 = diag(m_{11}, m_{22}, m_{33}). \\
&M_2 = diag(m_{44}, m_{55}, m_{66}).
\end{aligned} \tag{4}$$

where the positive constant terms $m_{jj}, 1 \le j \le 6$, denote the vehicle mass including added mass in surge(x), sway(y), heave(z), pitch and yaw. The Coriolis matrices are

$$C_1(v_1) \equiv \begin{bmatrix} 0 & m_{33}w & -m_{22}v \\ -m_{33}w & 0 & m_{11}u \\ m_{22}v & -m_{11}u & 0 \end{bmatrix} \tag{5}$$

$$C_2(v_2) \equiv \begin{bmatrix} 0 & m_{66}r & -m_{55}q \\ -m_{66}r & 0 & m_{44}p \\ m_{55}q & -m_{44}p & 0 \end{bmatrix} \tag{6}$$

The damping matrices are

$$D_1(v_1) = diag\left(d_{11} + \sum_{i=2}^{3} d_{ui} \mid u \mid^{i-1}, d_{22} + \sum_{i=2}^{3} d_{vi} \mid v \mid^{i-1}, d_{33} + \sum_{i=2}^{3} d_{wi} \mid w \mid^{i-1} \right) \tag{7}$$

$$D_2(v_2) = diag\left(d_{44} + \sum_{i=2}^{3} d_{pi} \mid p \mid^{i-1}, d_{55} + \sum_{i=2}^{3} d_{qi} \mid q \mid^{i-1}, d_{66} + \sum_{i=2}^{3} d_{ri} \mid r \mid^{i-1} \right) \tag{8}$$

where $d_{jj}, d_{ui}, d_{vi}, d_{wi}, d_{pi}, d_{qi}, d_{ri}$ and $1 \le j \le 6, i = 2,3$, represent the hydraulic-dynamic damping in surge, sway, heave, roll, pitch and yaw. The restoring force vector is

$$g_2(\eta_2) = [\rho g \nabla GM_T \sin(\phi) \quad \rho g \nabla GM_L \sin(\theta) \quad 0]^T \tag{9}$$

where ρ, g, ∇, GM_T *and* GM_L are the water density, gravity acceleration, displaced volume of water, transverse metacentric height and longitudinal metacentric height; respectively. The available inputs are

$$\tau_1 = [\tau_u \quad 0 \quad 0]^T, \quad \tau_2 = [\tau_p \quad \tau_q \quad \tau_r]^T \tag{10}$$

where τ_u, τ_p, τ_q *and* τ_r are the control force in surge and torques in roll, pitch and yaw; respectively. They are applied from two counter direction propellers actuated by electric motors and four cruciform tail fins($\delta_1, \delta_2, \delta_3, \delta_4$) at 0°, 90°, 180°, 270°.

The relationship between rolling/pitching/ yawing channel actuating angles ($\delta p, \delta q, \delta r$) and four fin angles ($\delta_1, \delta_2, \delta_3, \delta_4$) is

$$\begin{bmatrix} \delta p \\ \delta q \\ \delta r \end{bmatrix} = \begin{bmatrix} 1/2 & 0 & 1/2 & 0 \\ 0 & 1/2 & 0 & -1/2 \\ -1/2 & 0 & 1/2 & 0 \end{bmatrix} \begin{bmatrix} \delta_1 \\ \delta_2 \\ \delta_3 \\ \delta_4 \end{bmatrix}; \quad \begin{bmatrix} \delta_1 \\ \delta_2 \\ \delta_3 \\ \delta_4 \end{bmatrix} = \begin{bmatrix} 1 & 0 & -1 \\ 0 & 1 & 0 \\ 1 & 0 & 1 \\ 0 & -1 & 0 \end{bmatrix} \begin{bmatrix} \delta p \\ \delta q \\ \delta r \end{bmatrix} \tag{11}$$

The small-signal perturbation models of three angular rates (p,q,r) and two accelerations ($\dot{w},\dot{v}$) from control efforts ($\delta p, \delta q, \delta r$) for different operating speed ($V_m = \sqrt{u^2 + v^2 + w^2}$ in m/s) around trims $(\alpha, \beta) = (0°, 0°)$ are given below:

$$\begin{aligned}
&\frac{p}{\delta p} = \frac{p_n V_m^2}{s + p_d V_m}; \\
&\frac{q}{\delta q} = \frac{q_{n1} V_m^2 s - q_{n0} V_m^3}{s^2 + q_{d1} V_m s - q_{d0} V_m^2}; \quad \frac{r}{\delta r} = \frac{-r_{n1} V_m^2 s - r_{n0} V_m^3}{s^2 + r_{d1} V_m s - r_{d0} V_m^2}; \\
&\frac{\dot{w}}{\delta q} = \frac{-w_{n2} V_m^2 s^2 + w_{n1} V_m^3 s + w_{n0} V_m^4}{s^2 + w_{d1} V_m s - w_{d0} V_m^2}; \\
&\frac{\dot{v}}{\delta q} = \frac{+v_{n2} V_m^2 s^2 - v_{n1} V_m^3 s - v_{n0} V_m^4}{s^2 + v_{d1} V_m s - v_{d0} V_m^2}
\end{aligned} \tag{12}$$

All coefficients given in Eq.(12) are positive values. They give the considered system is an unstable open-loop system in pitching and yawing channels. Therefore, they need stable compensation and gain adaptation for autopilot according to the vehicle speed (V_m).

The vehicle will approach to a steady-state speed (V_{ms}) after the propelling force and drag are balanced. That is, a rolling speed of propelling motor (M_{spd}) corresponding to a steady-state vehicle speed (V_{ms}). The steady-state speed (V_{ms}) must be modified by amplitudes of pitching and yawing angular rates for lager drag will be get for large angle of attack and sideslip(α,β). It is in the form of

$$V_{ms} = a_0 + a_1|r'| + a_2|r'^2| + a_3|r'^3| \text{(m/s)} \qquad (13)$$

where $r' \equiv \sqrt{r^2+q^2}$ and a_i are functions of M_{spd}. They are evaluated from theoretical calculations, 6-DOF simulations and corrected by real navigation experiments. Fig. 2 shows relationships between M_{Spd}, V_{ms} and *r'* of the considered system. It shows the larger value of *r'*, the less value of vehicle speed. Eq.(13) gives the steady-state conditions and can be used to formulate the completely propelling dynamic model of vehicle speed form motor speed command (M_{TCmd}). Two dynamic models will be added to describe the motor speed response and the water compressibility. They are represented by two first-order models:

$$\frac{M_{spd}}{M_{TCmd}}(s) = \frac{1}{1+1.353s}; \quad \frac{V_m}{V_{ms}}(s) = \frac{1}{1+1.175s} \qquad (14)$$

Time constants (1.353, 1.175) given in Eq. (14) are all evaluated and verified by post data processing of navigation experiments. Eqs. (13)-(14) describe the open-loop speed response from motor speed command. In this work, open-loop speed control will be used for there is no speedometer in AUV. The time responses of the vehicle speed from motor speed command will be illustrated in Section 5.

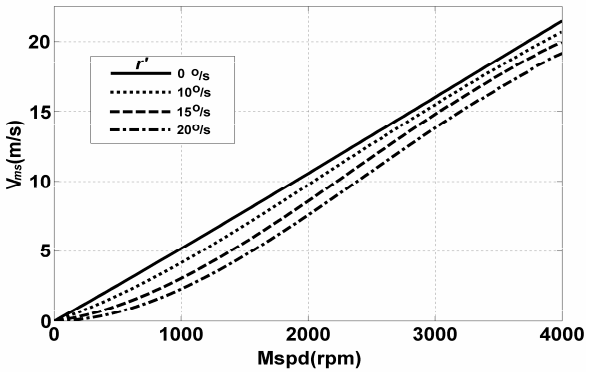

Figure 2. Steady-state relationships between V_{ms}, M_{Spd} and total angular rate *r'*.

3 Control configuration and adaptive autopilot designs

The control configuration of the considered autonomous underwater vehicle (AUV) is shown in Fig.3. It is a rolling stabilized control with skid-to-turn maneuver[10]. Control laws provide a stable controlled vehicle to be guided and variable control structures are ready to be selected for different guidance laws [11]. The yawing control law provides angular and angular rate controls to be selected. The pitching control law provides angular and depth controls to be selected. Note that the dashed-arrow lines represent gains: Kop, Kip, Kh, Koq, Kiq, Kor, Kir; and angular rate/ angular limits: $p_{\lim}, q_{\lim}, r_{\lim}, \theta_{\lim}$ are adapted according to vehicle speed (V_m). The updating rate of them is 20Hz. The purpose of them is to keep angle of attack/sideslip within in eight degrees for small drag and vehicle stability. For instance, small values of $p_{\lim}, q_{\lim}, r_{\lim}, \theta_{\lim}$ will be used for low-speed to prevent large angle of attack/sideslip operation.

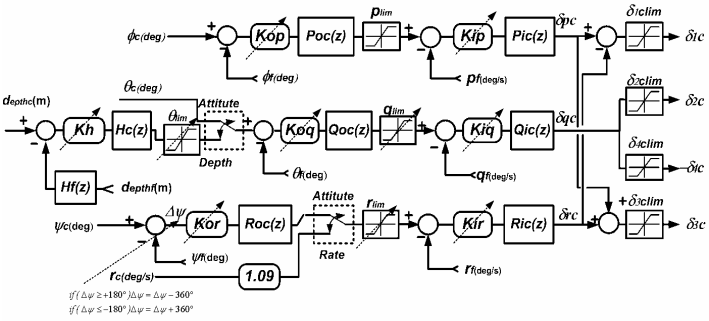

Figure 3. Adaptive and variable structure autopilot configuration.

Design results of compensators, adaptive gains and rate limits shown in Fig.3 are all given below:

(a) Rolling Channel gains and compensators:

$$Poc(z) = \frac{0.3333z - 0.2065}{z - 0.8732}; \quad Pic(z) = \frac{5.00z - 4.233}{z - 0.2231};$$

$$Kop = -0.0039V_m^{\,2} + 0.1523V_m + 2.719;$$

$$Kip = +0.0110V_m^{\,2} - 0.3999V_m + 3.927; \quad p_{\lim} = 45°/s.$$

(b) Yawing Channel gain and compensators:

$$Roc(z) = \frac{0.5z - 0.4391}{z - 0.9391}; \; Ric(z) = \frac{18.44z^2 - 32.92z + 14.736}{z^2 - 1.290z + 0.3279};$$

$$Kor = +0.0021V_m^{\,2} + 0.0512V_m + 0.4271;$$

$$Kir = +0.0107V_m^{\,2} - 0.3932V_m + 3.954;$$

$r_{\lim} = 0.972V_m + 5.000$.

(c)Depth, Pitching Channel gains and compensators:

$$Hc(z) = \frac{0.8422z - 0.8343}{z^2 - 1.782z + 0.7902};\quad Hf(z) = \frac{0.0582}{z - 0.9418};$$

$$Qoc(z) = \frac{0.5z - 0.4391}{z - 0.9391};\quad Qic(z) = \frac{18.44z^2 - 32.92z + 14.736}{z^2 - 1.290z + 0.3279};$$

$$Kh = -0.0003V_m{}^2 - 0.0324V_m + 1.878;$$

$$\theta_{\lim} = +0.0333V_m{}^2 - 2.841V_m + 58.775;$$

$$Koq = +0.0021V_m{}^2 + 0.0512V_m + 0.4271;$$

$$Kiq = +0.0107V_m{}^2 - 0.3932V_m + 3.954;$$

$$q_{\lim} = 0.972V_m + 5.000$$

(d)Fin actuating limits:

$$\delta_{1c\lim} = 25°,\ \delta_{2c\lim} = 25°,\ \delta_{3c\lim} = 25°,\ \delta_{4c\lim} = 25°$$

They are evaluated from the small-signal dynamic model described by Eq.(12) and verified by 6-DOF simulations and navigation experiments. Note that the subtraction of yawing angular command ψ_c and feedback ψ_f shown in Fig.3 is formulated as in the form of

$$\begin{aligned} &\Delta\psi = \psi_c - \psi_f \\ &if\,(\Delta\psi \ge +180°)\Delta\psi = \Delta\psi - 360° \\ &if\,(\Delta\psi \le -180°)\Delta\psi = \Delta\psi + 360° \end{aligned} \qquad (15)$$

to get proper sign of yawing angular rate control for domains of ψ_c and ψ_f are in $(0°,360°)$. The performances of depth and yawing angle controls will be illustrated by experimental results given in Section 5.

4 Vehicle position estimation method

4.1 Positioning analyses of the INS

For pure INS, lateral deviations (Δy_{gyro}, $\Delta y_{\Delta\phi\_ini}$, Δy_{acc_err}) due to rolling gyro drift (ϕ_{drift}), rolling installing error($\Delta\phi_{ini}$), and accelerometer accuracy(acc_{err}) versus time t are given below [5]:

$$\begin{aligned} \Delta y_{gyro} &= (1/6)\times 9.8\times \phi_{drift}\times t^3/57.296 \text{ m}; \\ \Delta y_{\Delta\phi\_ini} &= (1/2)\times 9.8\times \Delta\phi_{ini}\times t^2/57.296 \text{ m}; \\ \Delta y_{acc\_err} &= (1/2)\times acc_{err}\times t^2 \text{ m} \end{aligned} \qquad (16)$$

The total lateral deviation is the root sum square of three deviation terms. For limited budget, the specifications of the INS used in the considered AUV are: (a) Installation accuracy (3σ): in $0.05deg$; (b) Gyro accuracy (3σ): bias drift in $0.05deg/hr$; (c) accelerometer accuracy (3σ): in $0.15mg$. For example: (a) $\Delta y_{gyro} = 288.6m$ for $\phi_{drift} = 0.05\text{deg}/hr$ and $t = 900\text{sec}$; (b) $\Delta y_{gyro} = 18{,}471m$ for $\phi_{drift} = 0.05\text{deg}/hr$ and $t = 3{,}600\text{sec}$; (c) $\Delta y_{acc\_err} = 595.3m$ for $0.15mg$ and $t = 900\text{sec}$; (d) $\Delta y_{acc\_err} = 9{,}525m$ for $acc_{err} = 0.15mg$ and $t = 3{,}600\,sec$;. They give the accelerometer accuracy gives larger lateral deviation than that of gyro accuracy and deviations become unacceptable after time is greater than 900sec. Therefore, other positioning techniques must be applied for getting a non-diverging position datum for long-time underwater applications.

4.2 The proposed positioning method without state observers

Two bounded datum and three low-drift attitude angles ϕ,θ, and ψ of INS can be used to improving positioning of the AUV. The bounded datum are the speed of the propelling motor (M_{spd}) and the depth measurement from depth meter (d_{epthf}). Assume that V_{mest} is the estimated vehicle speed with respect to sea current, and (V_{west}, ψ_w) are estimated magnitude and course of the sea current with respect to ground. Then, the estimated vehicle speed $[V_{est}, V_{est}, V_{est}]^t$ with respect to ground along the inertial axes is in the form of

$$\begin{bmatrix} V_{xest} \\ V_{yest} \\ V_{zest} \end{bmatrix} \equiv \begin{bmatrix} c\theta_f c\psi_f & s\phi_f s\theta_f c\psi_f - c\phi_f s\psi_f & c\phi_f s\theta_f c\psi_f + s\phi_f s\psi_f \\ c\theta_f s\psi_f & c\phi_f c\psi_f + s\phi_f s\theta_f s\psi_f & c\phi_f s\theta_f s\psi_f - s\phi_f c\psi_f \\ -s\theta_f & s\phi_f s\theta_f & c\phi_f c\theta_f \end{bmatrix} \begin{bmatrix} V_{mest} \\ 0 \\ 0 \end{bmatrix}$$
$$+ \begin{bmatrix} c\psi_w \\ s\psi_w \\ 0 \end{bmatrix} V_{west} \equiv J_1(\eta_{2f}) \begin{bmatrix} V_{mes}t \\ 0 \\ 0 \end{bmatrix} + J_1(\eta_w) \begin{bmatrix} V_{west} \\ 0 \\ 0 \end{bmatrix} \qquad (17)$$

where $\eta_{2f} = [\phi_f \quad \theta_f \quad \psi_f]^T$ and $\eta_w = [0 \quad 0 \quad \psi_w]^T$. The total velocity ($V_{mt}$) of the vehicle is defined as the root sum square of velocity components. Integrations of them give the estimated vehicle position $[X_{est}, Y_{est}, Z_{est}]^t$. They are given below:

$$\begin{aligned} &Z_x(k+1) = T\times V_{xest} + Z_x(k); X_{est} = Z_x(k+1); \\ &Z_y(k+1) = T\times V_{yest} + Z_y(k); Y_{est} = Z_y(k+1); \\ &Z_z(k+1) = T\times V_{zest} + Z_z(k); Z_{est} = Z_z(k+1) \end{aligned} \qquad (18)$$

where $Z_x(k), Z_y(k), Z_z(k)$ are state variables of integrations with initial states specified. The computation period $T = 10ms$.

The estimated vehicle speed (V_{mest}) is derived

from steady-state speed (V_{est}) described by Eq. (13) plus the dynamics of the propelling motor and compress of seawater described by Eq. (14). They are transformed to Z-domain descriptions [12]. The motor speed command M_{TCmd} (rpm) is the input and the output of the estimated result is V_{mest} (m/s). The relationships between M_{TCmd}, V_{est} and V_{mest} are given below:

$$Z_m(k+1) = 0.0074 \times M_{TCmd} + 0.9926 \times Z_m(k); M_{spd} = Z_m(k+1) \quad (19)$$

$$V_{est} = S_{cvm}(a_0 + a_1|r''| + a_2|r''^2| + a_3|r''^3|) \quad (20)$$

$$Z_v(k+1) = 0.0085 \times V_{est} + 0.9915 \times Z_v(k); V_{mest} = Z_v(k+1) \quad (21)$$

where $r'' \equiv \sqrt{r_f{}^2 + q_f{}^2}$ and r_f, q_f are yawing/ pitching angular rates measured by INS. S_{cvm} is the correction factor. Default value of S_{cvm} is 1.00 and calibrated according the operating area.

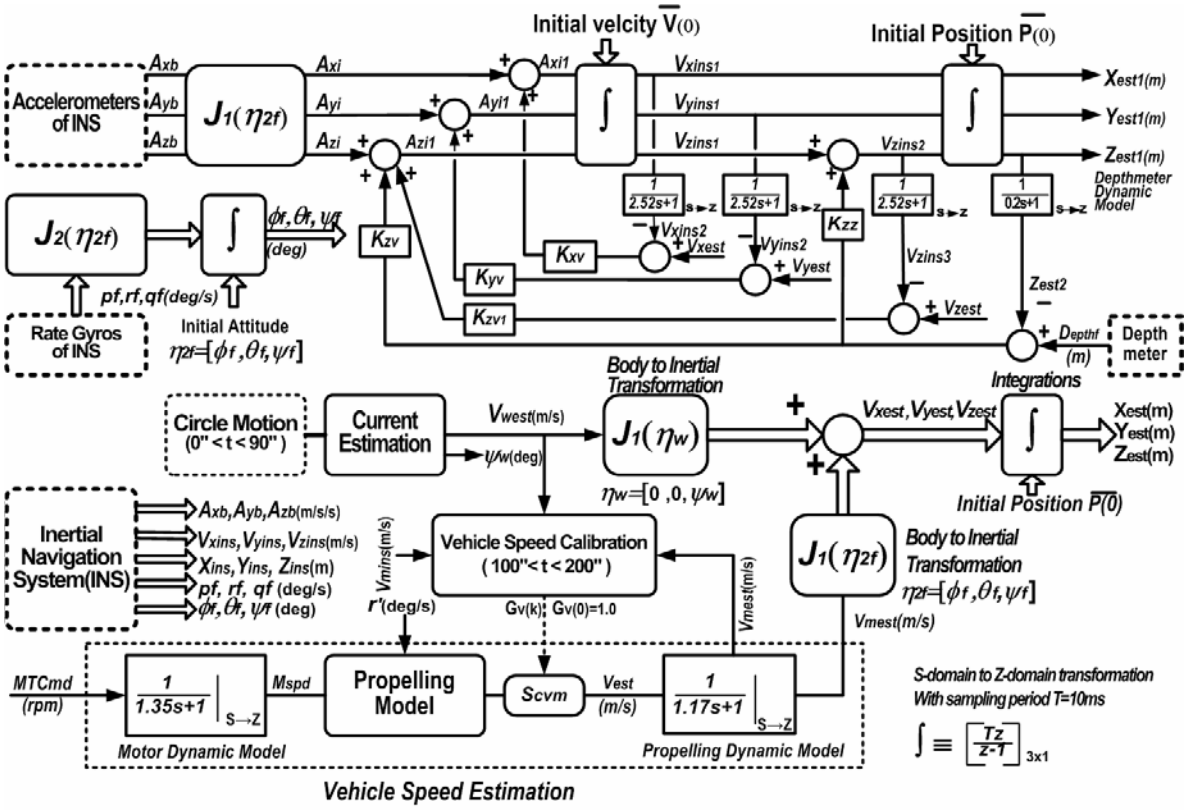

Figure 4. The proposed vehicle position estimation scheme.

The sea current estimation is derived from a constant-yawing angular rate, speed and depth motion. Note that circle motion can get the desired current datum with regardless the vehicle speed will be. The position deviation between start and end of the 360 degrees circle motion will give the current amplitude and course. The position datum (X_m, Y_m, Z_m) is get from INS for short-time inaccuracy is negligible. Equations for current estimation are

$$(\Delta_x, \Delta_y, \Delta_z) = (X_m, Y_m, Z_m)|_{T_o + to} - (X_m, Y_m, Z_m)|_{to} \quad (22)$$

$$V_{west} \equiv \sqrt{\Delta_x{}^2 + \Delta_y{}^2}/T_o; \psi_w = a\tan 2(\Delta_y, \Delta_x) \times 57.3 \quad (23)$$

where t_o is the starting time, r_c is the yawing angular rate and period $T_o = 360/r_c$, V_{west} and ψ_w is the estimated current speed and course with respect to the truth north(0°).

Once the estimation of sea current is obtained, the vehicle speed described by Eq. (20) can be further calibrated by following on-line adaptive law:

$$G_v(k+1) = G_v(k) \times [\gamma \sqrt{V_{mest}{}^2 + V_{west}{}^2}/V_{mins} + (1-\gamma)]; \quad S_{cvm} = G_v(k+1); \quad (24)$$

where $G_v(0) = 1$, $\gamma = 0.8$ and $V_{mins} = \sqrt{V_{xins}{}^2 + V_{yins}{}^2 + V_{zins}{}^2}$ is evaluated from three axis velocity components measured by INS. The ratio of $G_v(k+1)/G_v(k)$ will be converged to be unity after $V_{mins} \equiv \sqrt{V_{mest}{}^2 + V_{west}{}^2}$.

The calibrating process is performed at beginning navigation after current is estimated for position drift of INS is still acceptable. The positioning technique stated is shown in the lower part of Fig.4. It is an open-loop positioning process.

4.3 The proposed positioning method with state observers

The open-loop positioning process can be further improved by state observers [13] shown in the upper part of Fig.4. The datum used for position accuracy improvement are accelerations of body-axis (A_{xb}, A_{yb}, A_{zb}), depth measurement (d_{epthf}), estimated velocity components ($V_{xest}, V_{yest}, V_{zest}$) described by Eq. (18). The dynamic model of the depth meter $1/(0.2s+1)$ and vehicle speed dynamic model $1/(2.52s+1)$ are used in state observers for data synchronization. They are also transformed to Z-domain descriptions. $K_{zv}, K_{zz}, K_{zv1}, K_{yv}, K_{xv}$ are observer gains. Equations of the position estimation with state observers are given below:

$$\begin{bmatrix} A_{xi} \\ A_{yi} \\ A_{zi} \end{bmatrix} \equiv J_1(\eta_{2f}) \begin{bmatrix} A_{xb} \\ A_{yb} \\ A_{zb} \end{bmatrix} \tag{25}$$

where $\eta_{2f} = \begin{bmatrix} \phi_f & \theta_f & \psi_f \end{bmatrix}^T$, (A_{xb}, A_{yb}, A_{zb}) are accelerations along the body axes; A_{xi}, A_{yi}, A_{zi} are accelerations along the inertial axes. (A_{xi}, A_{yi}, A_{zi}) are corrected and double integrated to get the estimated position datum ($X_{est1}, Y_{est1}, Z_{est1}$) along the inertial axes. Certainly, better accuracy of ($X_{est1}, Y_{est1}, Z_{est1}$) is expected than that of ($X_{est}, Y_{est}, Z_{est}$). The attitude angles (ϕ_f, θ_f, ψ_f) are evaluate from the angular rates (p_f, q_f, r_f). They are in the form of

$$\begin{bmatrix} \dot{\phi}_f \\ \dot{\theta}_f \\ \dot{\psi}_f \end{bmatrix} \equiv J_2(\eta_{2f}) \begin{bmatrix} p_f \\ q_f \\ r_f \end{bmatrix} \tag{26}$$

and

$$\begin{aligned} Z_p(k+1) &= T \times \dot{\phi}_f + Z_p(k); \phi_f = Z_p(k+1); \\ Z_q(k+1) &= T \times \dot{\theta}_{ft} + Z_q(k); \theta_f = Z_q(k+1); \\ Z_r(k+1) &= T \times \dot{\psi}_f + Z_r(k); \psi_f = Z_r(k+1) \end{aligned} \tag{27}$$

where $Z_p(k), Z_q(k), Z_r(k)$ are state variables of integrations with initial states specified, and $J_2(\bullet)$ is defined by Eq. (3). The accelerations (A_{xi}, A_{yi}, A_{zi}) are corrected by three velocity and one depth differences as in the form of

$$\begin{aligned} A_{xi1} &= A_{xi} + K_{xv} \times (V_{xest} - V_{xins2}); \\ A_{yi1} &= A_{yi1} + K_{yv} \times (V_{yest} - V_{yins2}); \\ A_{zi1} &= A_{zi1} + K_{zv} \times (V_{zest} - V_{zins3}) + K_{zv1} \times (d_{epthf} - Z_{est2}); \end{aligned} \tag{28}$$

Integrations of (A_{xi}, A_{yi}, A_{zi}) gives ($V_{xins1}, V_{yins1}, V_{zins1}$). Equations of integration are given below:

$$\begin{aligned} Z_{vx}(k+1) &= T \times A_{xi1} + Z_{vx}(k); V_{xins\,1} = Z_{vx}(k+1); \\ Z_{vy}(k+1) &= T \times A_{yi1} + Z_{vy}(k); V_{yins1} = Z_{vy}(k+1); \\ Z_{vz}(k+1) &= T \times A_{zi1} + Z_{vz}(k); V_{zins1} = Z_{vz}(k+1); \end{aligned} \tag{29}$$

where $Z_{vx}(k), Z_{vy}(k), Z_{vz}(k)$ are state variables of integrations with initial states specified. The terms ($V_{xins2}, V_{yins2}, V_{zins3}, Z_{est2}$) given in Eq. (28) are evaluated as following expressions:

$$\begin{aligned} Z_{mx}(k+1) &= 0.0488 \times V_{x\sin 1} + 0.9512 \times Z_{mx}(k); V_{xins2} = Z_{mx}(k+1); \\ Z_{my}(k+1) &= 0.0488 \times V_{x\sin 1} + 0.9512 \times Z_{my}(k); V_{xins2} = Z_{my}(k+1); \\ Z_{mz}(k+1) &= 0.0488 \times V_{x\sin 2} + 0.9512 \times Z_{mz}(k); V_{xins3} = Z_{mz}(k+1); \\ Z_{dz}(k+1) &= 0.0040 \times X_{est1} + 0.9960 \times Z_{mx}(k); Z_{est2} = Z_{dz}(k+1); \end{aligned} \tag{30}$$

where $Z_{mx}(k), Z_{my}(k), Z_{mz}(k), Z_{de}(k)$ are state variables with initial states specified. The term V_{zins1} is corrected by depth differential.

$$V_{zins2} = V_{zins1} + K_{zz} \times (d_{epthf} - Z_{est2}) \tag{31}$$

for only depth data can be used. Integrations of ($V_{xins1}, V_{yins1}, V_{zins2}$) gives position ($X_{est1}, Y_{est1}, Z_{est1}$).

$$\begin{aligned} Z_x(k+1) &= T \times V_{xins1} + Z_x(k); X_{est\,1} = Z_x(k+1); \\ Z_y(k+1) &= T \times V_{yins1} + Z_y(k); Y_{ests1} = Z_y(k+1); \\ Z_z(k+1) &= T \times V_{zins2} + Z_z(k); Z_{est1} = Z_z(k+1); \end{aligned} \tag{32}$$

where $Z_x(k), Z_y(k), Z_z(k)$ are state variables of integrations with initial states specified. The observer gains $K_{zv}, K_{zz}, K_{zv1}, K_{yv}, K_{xv}$ are found as $K_{zv} = 0.05$, $K_{zz} = 0.50$, $K_{zv1} = 0.10$, $K_{yv} = 0.10, K_{xv} = 0.10$.

5 Experimental Results

5.1 Experimental planning

The proposed positioning technique was verified by two experiments. The average depth of the seabed is 78m. Fig.5 shows a testing plan of the navigation experiment with the launching point is located at (119°49’35”E, 22°39’50”N). Six transponders (A-F) at the seabed and one transponder in the vehicle are used for

long-baseline acoustic positioning system (LBL). Positions of six transponders at the seabed are corrected by GPS in installation. Antennas are connected to the transponders by cables for transmitting distances between transponders to data processing center. The position error of the transponder is within 5m. Therefore, the best accuracy of the LBL is within 5m. Two sound sources for sonar tracking are installed at W_{p1} and W_{p2} with 30m depth. This experiment was planned for active and passive sonar target tracking. The passive target sound source was put at W_{p1} and the active target sound source was put at W_{p2}. The angle between tacking locus and line of sight (LOS) is 15degree for safety consideration of crew in the launching vehicle. The vehicle was navigated to and fro alternatively between waypoints W_{p1} and W_{p2} by locus tracking control law. The vehicle will change course at the situation of distance between vehicle and W_{p1}(or W_{p2}) is equal to 200m. The vehicle course is determined by tracking locus described by $\overline{W_{p1}W_{p2}}$ or $\overline{W_{p2}W_{p1}}$. The locus tracking control law is proposed and discussed in detail in Appendix A.

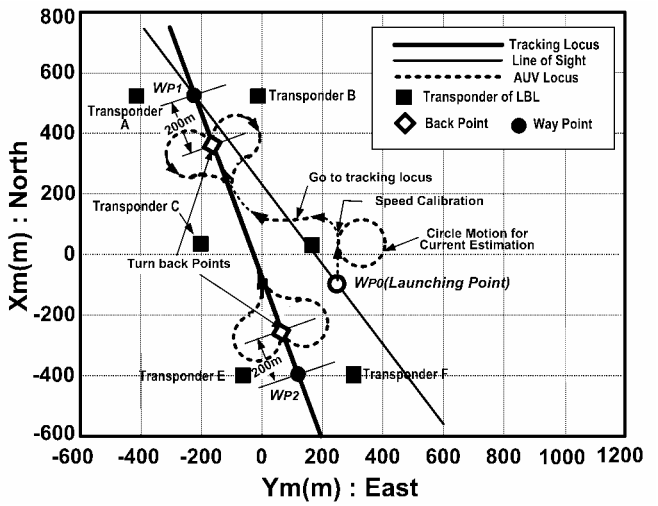

Figure 5. Mission Planning for AUV Navigation Testing.

5.2 Experimental results

The circle motion for current estimation gives the estimated results was $(V_{west}, \psi_w) = (0.19m/s, 291\text{deg})$ The calibration factor S_{cvm} for the vehicle speed is 1.05. Fig.6 shows the vehicle speed responses and comparisons between proposed estimated and LBL results. The LBL datum is raw datum without low-pass filtering. Therefore, they are fluctuating. However, from averages of them one can see the responses modeling of vehicle speed described by Eqs.(13) and (14) give good agreement with the LBL results.

Fig.7 shows the vehicle depth responses and comparisons between depth command, depth meter and TBL. They give good agreements between them and good depth control performance.

Fig.8 shows the deviations (solid-line) between the estimated position (X_{est1}, Y_{est1}) and the tracked datum. It gives the maximal deviation is 33.6m and the average deviation is 15.1m. They are much less than the detecting ranges of the sonar in the shallow water. The errors (doted- line) of proposed method without state observer are shown in Fig.8 also. It gives the maximal deviation is 61.3m and the average deviation is 25.2m.

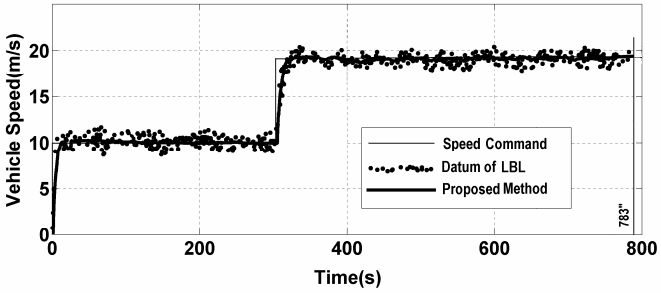

Figure 6. Vehicle speed time responses.

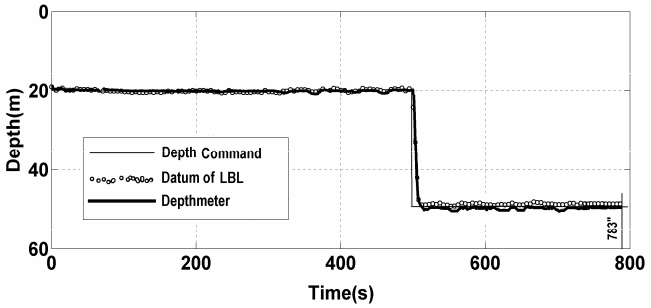

Figure 7. Vehicle depth time responses.

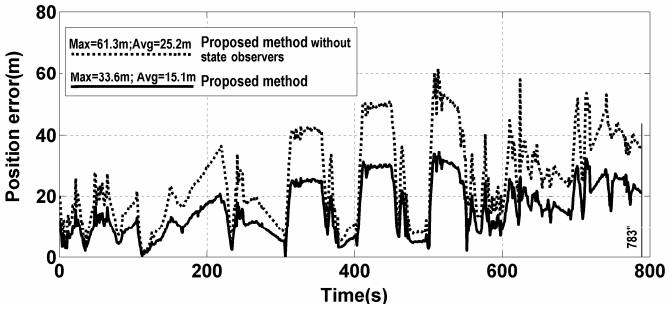

Figure 8. Position errors with respect to LBL.

Note that the position datum of the INS with the specification stated in Section 4. It gives maximal deviation 524m from the tracking locus. This deviation is greater than that of the detection range of sonar in the shallow water. Note that the launching vehicle is dangerous if the position datum of INS were used for locus tracking. Note also that greater deviation will be obtained for the operation time greater than 13mins. Eq. (16) gives the deviation will become unacceptable for one-hour operation.

5.3. Another experimental results

Fig.9 shows mission planning for large area underwater target searching and control performance verification. The current estimation gave $(V_{west}, \psi_w) = (0.24m/s, 151\deg)$. The calibration factor S_{cvm} for vehicle speed is 1.06. The position deviation with respect to LBL datum is shown in Fig.10. The maximal deviation is 25.6m and the average deviation is 11.8m for 1176sec(19.6mins) underwater operation. From comparison results shown in Figs. 8 and 10, one can see the proposed method gives good and non-diverging positioning and ready for long-time operation without correction from LBL or GPS. The installation of LBL system was omitted in the next experiment.

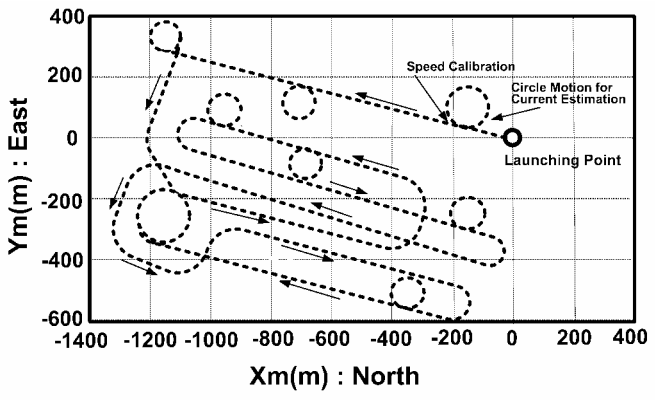

Figure 9. Mission planning for large area underwater target searching.

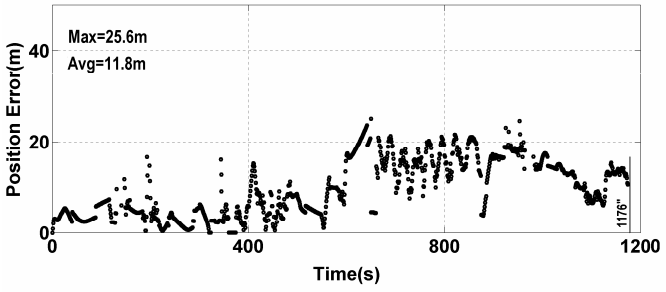

Figure 10. Position errors of another experiment with respect to LBL.

6 Conclusions

In this paper, an accurate positioning technique has been proposed for autonomous underwater vehicles (AUV). It needs not position correction from GPS above the sea surface and SBL or LBL under the sea. Rolling speed of the propelling motor, depth measurement of depth meter, estimated current information and low cost rate gyros and accelerometers with state observers were used to estimate the vehicle position. It gave less than 20m deviations for 13 minutes and 19.6 minutes underwater operations. The deviations were verified by a long-baseline acoustic position system (LBL) with positioning accuracy less than 5m. High accurate position lets the vehicle have flexible and mobile applications and less supporting from launching vessel.

References

[1] J. Yuh, Design and control of autonomous underwater robots: A Survey, *Autonomous Robots*, Vol.8, 2000, pp.7-24.

[2] D. Bingham, et al, The application of autonomous underwater vehicle (AUV) technology in oil industry-vision and experience, *FIG, XXII International Congress,* Washington DC, 2002.

[3] W. H. Cheng, A study of increasing the precision of navigation position for submerged body, *Ocean Engineering* Vol.31, 2004, pp.693-707.

[4] M. J. Morgan, Dynamic positioning of offshore vessels, Petroleum publishing Co. Tulsa, Oklahoma, 1978.

[5] J. A. Farrell, *The Global Positioning System & Inertial Navigation*, McGraw-Hill Professional, 1998.

[6] N. H. Kussat, C. D. Chadwell, Zimmerman, R., Absolute positioning of an autonomous underwater vehicle using GPS and acoustic measurements, *IEEE Journal of Oceanic Engineering*, Vol.30, 2005, pp.153-164.

[7] W. S. Burdic, *Underwater Acoustic System analysis*, Prentice-Hall, 1991.

[8] R. J., Urick, *Principles of Underwater Sound*, McGraw-Hill, 1993.

[9] T. I. Fossen, *Guidance and Control of Ocean Vehicles*, John Wiley & Sons, 1994.

[10]J. Garus, Design of Model Reference Adaptive Control for Underwater Robotic Vehicles,

WSEAS Transactions on Systems, Vol.5, No.11, 2006, pp.2562-2569.

[11]W. Naeem, R. Sutton, Ahmad, S.M. and Burns, R.S., A review of guidance laws applicable to unmanned underwater vehicles. *Journal of Navigation*, Vol. 56, 2003, pp.15-29.

[12]K.Ogata,*Discrete-time Control System*, Prentice-Hall Inc. Englewood Cliffs, NJ, 1994.

[13]G. F. Franklin, *Feedback Control of Dynamics*, Addison-Wesley Publishing Company, 1986.

Appendix A: Locus Tracking Law

The tracking locus connected with point # i (X_i, Y_i) and point # i+1 (X_{i+1}, Y_{i+1}) and tracking definition is formulated as following equations. The tracking locus is defined as

$$a_{i+1}X + b_{i+1}Y + c_{i+1} = 0 \qquad \text{(A1)}$$

with $a_{i+1} = Y_{i+1} - Y_i, b_{i+1} = X_{i+1} - X_i$ *and* $c_{i+1} = X_i Y_{i+1} + X_{i+1} Y_i$, the normal displacement between vehicle(X_M, Y_M) and the tracking locus is

$$LH = -(a_{i+1}X_M - b_{i+1}Y_M + c_{i+1}) / \sqrt{a_{i+1}^2 + b_{i+1}^2} \qquad \text{(A2)}$$

Positive value of *LH* represents the vehicle is on the right-hand side of the tracking locus; negative value of *LH* represents the vehicle is on the left-hand side of the tracking locus. The purpose of locus tracking is to keep *LH* be a wanted value (*LHc*); and moving from point #i toward point # i+1. *LHc*=0 represents the vehicle will moving on the tracking locus. The direction of the vehicle will move always from way point #i to way point # i+1 for controlled parameters are *LH=LHc* and $\psi_c = \psi_{c1}$; which is shown in Fig.A1. It shows the geometry relation of the vehicle and the tracking locus. For faster locus tracking purpose, variable structure control scheme is switched according to amplitude of LH. The vehicle will be guided toward to tracking locus orthogonally for |LH| > *R*, and toward to way point #i+1 for |LH| < R. The selection of R is the minimal turning radius capability of the vehicle at high speed maneuvering. It will perform smoothing tracking performance and low water flowing noise. The guidance law is formulated as

$$\psi_{c1} = 57.296 \times a\tan 2(a_{i+1}, b_{i+1}) \qquad \text{(A3)}$$

$$\psi_{c2} = \psi_{c1} + 90 \times sign(LH) \qquad \text{(A4)}$$

$$\psi_c = \psi_{c1} + 2(LHc - LH) \text{.....} for\ LH < R + LHc \qquad \text{(A5)}$$

$$\psi_c = \psi_{c2} \text{.....} for\ LH > R + LHc \qquad \text{(A6)}$$

where *R* represents the minimal turning radius of the vehicle.

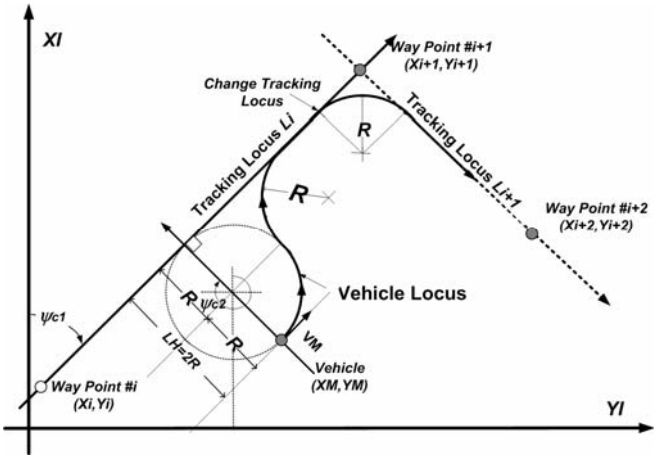

Figure A1. The fastest loci tracking concept with turning radius R.